Inorg. Chem. **2006**, *45*, 1032–1037

Three-Dimensional Nets from Star-Shaped Hexakis(arylthio)triphenylene Molecules and Silver(I) Salts

Kunhao Li,[†] Zhengtao Xu,*[,‡] Hanhui Xu,[†] Patrick J. Carroll,[§] and James C. Fettinger[||]

Department of Chemistry, The George Washington University, 725 21st Street NW, Washington, D.C. 20052, Department of Biology and Chemistry, City University of Hong Kong, 83 Tat Chee Avenue, Kowloon, Hong Kong, P. R. China, P. Roy and Diana T. Vagelos Laboratories, Department of Chemistry, University of Pennsylvania, 231 South 34th Street, Philadelphia, Pennsylvania 19104-6323, and Department of Chemistry and Biochemistry, University of Maryland, College Park, Maryland 20742

Received July 8, 2005

This article reports a number of functional 3D networks based on the coordination bonds between the silver(I) ion and polycyclic aromatic 2,3,6,7,10,11-hexakis(organylthio)triphenylene (HRTT) molecules. First, 2,3,6,7,10,11-hexakis-(phenylthio)triphenylene (HPhTT) chelates with $AgBF_4$ (or AgTf, where Tf is triflate) in the presence of hexafluorobenzene to form a 3D network (composition, HPhTT·AgBF4; space group, $I\bar{4}$), where each Ag(I) atom is bonded to three HPhTT molecules and acts as a three-connected node that interconnects the trigonal HPhTT ligands. In addition to the relatively rare 8^2·10-*a* topology, the network features distinct channel-like domains that incorporate various solvent molecules (e.g., acetone and tetrahydrofuran). The solvent molecules can be evacuated to produce a stable and crystalline apohost network, in which the solvent-accessible fraction of the cell volume is calculated to be about 16%. Second, chelation of 2,3,6,7,10,11-hexakis(4-methoxyphenylthio)triphenylene (HMOPhTT) and $AgSbF_6$ in a 1:1 ratio results in a 3D network featuring a similar 8^2·10-*a* topology and Ag(I) coordination environment. However, the crystallographic symmetry (space group *Cc*) is lowered, and the feature of porosity is much less distinct. The 3D networks show strong room-temperature fluorescence bands with $\lambda_{F,max} = 450$ nm, due to the π-electron fragment of the triphenylene group.

Introduction

In the rapidly growing field of extended coordination frameworks, it is of great interest to control and tailor the network structures so as to access the desired solid-state properties (or combinations of properties) such as porosity, network acentricity, fluorescence, and semiconductivity.[1−7] For example, the use of rigid and symmetrical molecular building units and secondary building units effectively constrains the local bonding geometry and can often lead to open-framework structures with various topologies and phenomena of interpenetration or porosity.[8−21] Also, the concept of minimal surface, initially developed for block

* To whom correspondence should be addressed. E-mail: zhengtao@cityu.edu.hk.
[†] The George Washington University.
[‡] City University of Hong Kong.
[§] University of Pennsylvania.
[||] University of Maryland.

(1) Janiak, C. *Dalton Trans.* **2003**, 2781.
(2) James, S. L. *Chem. Soc. Rev.* **2003**, *32*, 276.
(3) Kesanli, B.; Lin, W. *Coord. Chem. Rev.* **2003**, *246*, 305.
(4) Yaghi, O. M.; O'Keeffe, M.; Ockwig, N. W.; Chae, H. K.; Eddaoudi, M.; Kim, J. *Nature* **2003**, *423*, 705.
(5) Batten, S. R.; Robson, R. *Angew. Chem., Int. Ed.* **1998**, *37*, 1461.
(6) Batten, S. R.; Murray, K. S. *Coord. Chem. Rev.* **2003**, *246*, 103.
(7) Ockwig, N. W.; Delgado-Friedrichs, O.; O'Keeffe, M.; Yaghi, O. M. *Acc. Chem. Res.* **2005**, *38*, 176.
(8) Sun, H.-L.; Ma, B.-Q.; Gao, S.; Batten, S. R. *Cryst. Growth Des.* **2005**, *5*, 1331.
(9) Tong, M.-L.; Chen, X.-M.; Batten, S. R. *J. Am. Chem. Soc.* **2003**, *125*, 16170.
(10) Batten, S. R. *CrystEngComm.* **2001**, *18*, 1.
(11) Carlucci, L.; Ciani, G.; Proserpio, D. M.; Sironi, A. *Chem. Commun.* **1996**, 1393.
(12) Carlucci, L.; Ciani, G.; Proserpio, D. M.; Rizzato, S. *Dalton Trans.* **2000**, 3821.
(13) Carlucci, L.; Ciani, G.; Proserpio, D. M. *CrystEngComm.* **2003**, *5*, 269.
(14) Carlucci, L.; Ciani, G.; Proserpio, D. M.; Porta, F. *CrystEngComm.* **2005**, *7*, 78.
(15) Pan, L.; Liu, H.; Kelly, S. P.; Huang, X.; Olson, D. H.; Li, J. *Chem. Commun.* **2003**, 854.
(16) Pan, L.; Liu, H.; Lei, X.; Huang, X.; Olson, D. H.; Turro, N. J.; Li, J. *Angew. Chem., Int. Ed.* **2003**, *42*, 542.
(17) Pan, L.; Huang, X.; Phan, H.-L. N.; Emge, T. J.; Li, J.; Wang, X. *Inorg. Chem.* **2004**, *43*, 6878.

10.1021/ic051135e CCC: $33.50
Published on Web 01/06/2006

Chart 1

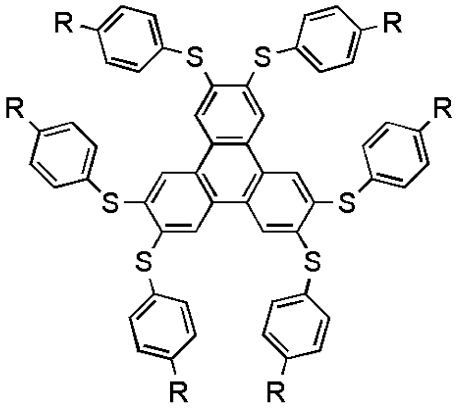

HPhTT R = -H

HMOPhTT R = -OCH_3

copolymers and liquid crystals, has recently proven an effective global model for structure rationalization and prediction of extended networks as well as other small-molecule systems.[22−24] As for acentric/homochiral crystals, Lin and co-workers have extensively investigated the use of unsymmetrical ligands to effectively enforce local as well as global acentricity in metal−organic frameworks in order to achieve nonlinear optical properties and enantioselective catalysis in the solid state.[25−31]

One of our approaches to access functional extended frameworks is based on star-shaped organic ligands containing large π-electron systems such as the 2,3,6,7,10,11-hexakis(organylthio)triphenylene molecules (HRTT, see Chart 1 for examples). As building blocks for metal−organic frameworks, such molecules offer certain advantages. For example, star-shaped molecules such as HRTT adopt open and radiant conformations that tend to obstruct close packing of the molecules, leaving empty space that can incorporate various guest molecules. Indeed, star-shaped molecules such as hexakis(phenylthio)benzene were originally studied for their versatile ability as hosts to incorporate guest molecules,[32,33] and more sophisticated systems have subsequently been reported.[34−42] Notably, star-shaped molecules have also entered into the field of crystalline networks for accessing porous or pocket-containing structures, where a wide range of diffusion or host−guest interaction phenomena could potentially be investigated within extended networks.[43−49]

Additionally, polycyclic aromatic ligands such as HRTT contain highly polarizable π-electron systems and can therefore help to accentuate important properties such as semiconductivity and fluorescence in the solid state. Recently, we reported a series of coordination networks based on 2,3,6,7,10,11-hexakis(organylthio)triphenylene (HRTT) ligands and inorganic components such as silver(I) triflate (AgTf) and bismuth(III) halides.[50−52] These network compounds featured various dimensionalities from 0D to 2D and rather well-defined correlation between the crystal structures and properties such as electronic band gaps and fluorescence emission intensity. One problem with these previous systems is the relatively low dimensionalities and poor stabilities of the host networks, which tend to collapse upon the evacuation of the solvent molecules. We have therefore been trying to achieve three-dimensional frameworks so as to impart more stability as well as potential porosity to these fluorescent/semiconductive frameworks. Reported here are a group of 3D coordination frameworks based on ligands of 2,3,6,7,-10,11-hexakis(phenylthio)triphenylene (HPhTT) and 2,3,6,7,-10,11-hexakis(4-methoxyphenylthio)triphenylene (HMOPhTT) (see Chart 1) and silver(I) salts. These network compounds feature the relatively rare topology of $8^2 \cdot 10$-*a* and contain various solvent molecules as guests. Preliminary studies

(18) Pan, L.; Sander, M. B.; Huang, X.; Li, J.; Smith, M.; Bittner, E.; Bockrath, B.; Johnson, J. K. *J. Am. Chem. Soc.* **2004**, *126*, 1308.
(19) Sudik, A. C.; Millward, A. R.; Ockwig, N. W.; Cote, A. P.; Kim, J.; Yaghi, O. M. *J. Am. Chem. Soc.* **2005**, *127*, 7110.
(20) Sudik, A. C.; Cote, A. P.; Yaghi, O. M. *Inorg. Chem.* **2005**, *44*, 2998.
(21) Chen, B.; Ockwig, N. W.; Fronczek, F. R.; Contreras, D. S.; Yaghi, O. M. *Inorg. Chem.* **2005**, *44*, 181.
(22) Chen, B. L.; Eddaoudi, M.; Hyde, S. T.; O'Keeffe, M.; Yaghi, O. M. *Science* **2001**, *291*, 1021.
(23) Xu, Z.; Kiang, Y.-H.; Lee, S.; Lobkovsky, E. B.; Emmott, N. *J. Am. Chem. Soc.* **2000**, *122*, 8376.
(24) Lee, S.; Mallik, A. B.; Xu, Z.; Lobkovsky, E. B.; Tran, L. *Acc. Chem. Res.* **2005**, *38*, 251.
(25) Lin, W.; Evans, O. R.; Xiong, R.-G.; Wang, Z. *J. Am. Chem. Soc.* **1998**, *120*, 13272.
(26) Cui, Y.; Evans, O. R.; Ngo, H. L.; White, P. S.; Lin, W. *Angew. Chem., Int. Ed.* **2002**, *41*, 1159.
(27) Evans, O. R.; Xiong, R. G.; Wang, Z. Y.; Wong, G. K.; Lin, W. *Angew. Chem., Int. Ed.* **1999**, *38*, 536.
(28) Evans, O. R.; Ngo, H. L.; Lin, W. *J. Am. Chem. Soc.* **2001**, *123*, 10395.
(29) Evans, O. R.; Lin, W. *Acc. Chem. Res.* **2002**, *35*, 511.
(30) Wu, C.-D.; Lin, W. *Angew. Chem., Int. Ed.* **2005**, *44*, 1958.
(31) Wu, C.-D.; Hu, A.; Zhang, L.; Lin, W. *J. Am. Chem. Soc.* **2005**, *127*, 8940−8941.
(32) Hardy, A. D. U.; MacNicol, D. D.; Wilson, D. R. *J. Chem. Soc., Perkin Trans. 2* **1979**, 1011.
(33) MacNicol, D.; Mallinson, P. R.; Murphy, A.; Sym, G. J. *Tetrahedron Lett.* **1982**, *23*, 4131.
(34) Gingras, M.; Pinchart, A.; Dallaire, C. *Angew. Chem., Int. Ed.* **1998**, *37*, 3149.
(35) Menger, F. M.; Azov, V. A. *J. Am. Chem. Soc.* **2002**, *124*, 11159.
(36) Walsdorff, C.; Saak, W.; Haase, D.; Pohl, S. *Chem. Commun.* **1997**, 1931.
(37) Yang, C.; Chen, X.-M.; Lu, X.-Q.; Zhou, Q.-H.; Yang, Y.-S. *Chem. Commun.* **1997**, 2041.
(38) Grube, G. H.; Elliott, E. L.; Steffens, R. J.; Jones, C. S.; Baldridge, K. K.; Siegel, J. S. *Org. Lett.* **2003**, *5*, 713.
(39) Tucker, J. H. R.; Gingras, M.; Brand, H.; Lehn, J.-M. *J. Chem. Soc., Perkin Trans. 2* **1997**, 1303.
(40) Gingras, M.; Pinchart, A.; Dallaire, C.; Mallah, T.; Levillain, E. *Chem. Eur. J.* **2004**, *10*, 2895.
(41) Mizyed, S.; Georghiou, P. E.; Bancu, M.; Cuadra, B.; Rai, A. K.; Cheng, P.; Scott, L. T. *J. Am. Chem. Soc.* **2001**, *123*, 12770.
(42) Pang, J.; Marcotte, E. J. P.; Seward, C.; Brown, R. S.; Wang, S. *Angew. Chem., Int. Ed.* **2001**, *40*, 4042.
(43) Suenaga, Y.; Kuroda-Sowa, T.; Maekawa, M.; Munakata, M. *Dalton Trans.* **2000**, 3620.
(44) Seward, C.; Jian, W.-L.; Wang, R.-Y.; Enright, G. D.; Wang, S. *Angew. Chem., Int. Ed.* **2004**, *43*, 2933.
(45) Goodgame, D. M. L.; Grachvogel, D. A.; White, A. J. P.; Williams, D. J. *Inorg. Chim. Acta* **2003**, *344*, 214.
(46) Goodgame, D. M. L.; Grachvogel, D. A.; Williams, D. J. *Inorg. Chim. Acta* **2002**, *330*, 13.
(47) Hoskins, B. F.; Robson, R.; Slizys, D. A. *Angew. Chem., Int. Ed.* **1998**, *36*, 2752.
(48) Kobayashi, K.; Shirasaka, T.; Sato, A.; Horn, E.; Furukawa, N. *Angew. Chem., Int. Ed.* **1999**, *38*, 3483.
(49) Suenaga, Y.; Konaka, H.; Kitamura, K.; Kuroda-Sowa, T.; Maekawa, M.; Munakata, M. *Inorg. Chim. Acta* **2003**, *351*, 379.
(50) Li, K.; Xu, Z.; Fettinger, J. C. *Inorg. Chem.* **2004**, *43*, 8018.
(51) Xu, Z.; Li, K.; Fettinger, J. C.; Li, J.; King, M. M. *Cryst. Growth Des.* **2005**, *5*, 423.
(52) Li, K.; Xu, Z.; Xu, H.; Ryan, J. M. *Chem. Mater.* **2005**, *17*, 4426.

Table 1. Selected Crystallographic Data for **1a**, **1b**, and **2**

	1a	1b	2
chem formula	$C_{111}H_{72}Ag_2B_2F_8OS_{12}$	$C_{55}H_{36}AgF_3O_3S_7$	$C_{121.5}H_{99}Ag_2F_{12}O_{12.5}S_{12}Sb_2$
fw	2195.77	1134.13	2830.97
space group	$I\bar{4}$	$I\bar{4}$	*Cc*
a, Å	20.1978(6)	20.1972(3)	25.279(2)
b, Å	20.1978(6)	20.1972(3)	30.237(2)
c, Å	25.032(1)	25.0091(7)	19.792(1)
α, deg	90	90	90
β, deg	90	90	128.401(1)
γ, deg	90	90	90
V, Å^3	10212.0(7)	10201.9(4)	11856(1)
Z	4	8	4
ρ_{calcd}, g/cm^3	1.428	1.477	1.586
wavelength, Å	0.71069 (Mo Kα)	0.71069 (Mo Kα)	0.71069 (Mo Kα)
abs coeff (μ), cm^{-1}	6.93	7.36	10.67
R1[a] [$I > 2s(I)$]	3.96%	3.37%	6.05%
wR2[b] [$I > 2s(I)$]	10.96%	9.26%	18.76%

[a] $R1 = \sum(||F_o| - |F_c||)/\sum(|F_o|)$. [b] $wR2 = \{\sum[w(F_o^2 - F_c^2)^2]/\sum[w(F_o^2)^2]\}^{1/2}$.

indicated improved network stability upon the evacuation of the solvent molecules. In addition, the extended structures all crystallized in noncentrosymmetric space groups, pointing to potential usefulness of these star-shaped molecules in forming acentric crystals.

Experimental Section

General Procedure. Starting materials, reagents, and solvents were purchased from commercial sources (Aldrich and Fisher Scientific) and used without further purification. The molecule 2,3,6,7,10,11-hexakis(phenylthio)triphenylene (HPhTT) was prepared from a reported procedure.[50] Melting points were measured on a Mel-temp II melting point apparatus (not corrected). Solution ^{1}H and ^{13}C NMR spectra were recorded on a 200-MHz Varian Mercury spectrometer at room temperature, with tetramethylsilane (TMS) as the internal standard. Photoluminescence measurements on the solid samples (ground with KBr and pressed into pellets) were performed on a Shimadzu RF-5301PC spectrofluorimeter at ambient temperature. X-ray diffraction patterns for the bulk samples were collected at room temperature on a Scintag XDS 2000 diffractometer (Cu Kα, $\lambda = 1.5418$ Å). The powder samples were pressed onto a glass slide for data collection. Thermogravimetric analysis (TGA) was performed on a Pyris TGA-1 instrument under flowing N_2 gas (20 mL/min) at a heating rate of 5 °C/min. Details of the X-ray diffraction studies on the single crystals are included in the Supporting Information, with selected crystallographic data presented in Table 1.

2,3,6,7,10,11-Hexakis(4-methoxyphenylthio)triphenylene (HMOPhTT). In an argon-filled glovebox, sodium hydride (anhydrous, 60% in mineral oil, 169 mg, 4.2 mmol) and hexabromotriphenylene (HBT, 200 mg, 0.29 mmol) were charged into a 25-mL two-neck round-bottom flask equipped with a septum. Under nitrogen protection, the flask was then connected to a vacuum manifold outside the glovebox, and 10 mL of 1,3-dimethyl-2-imidazolidinone (DMEU, 10 mL, 99%, anhydrous) was added via cannula. While the suspension was being stirred and chilled in an ice−water bath, 4-methoxythiophenol (97%, 0.42 mL, 3.4 mmol, purged with nitrogen for 2−3 min) was injected dropwise over 10 min.

The reaction mixture was stirred at room temperature for another 30 min and then heated to 60 °C for 4 h, after which the resultant yellow solution was poured into 100 mL of water and extracted with toluene (50 mL × 3). After the organic layers were combined, washed with water (200 mL × 3) and brine (200 mL, saturated), and dried with anhydrous sodium sulfate, the solvent was removed in vacuo, and the crude product was purified by flash chromatography (1:1 dichloromethane/hexanes) to yield a slightly yellow solid (263 mg, 87% based on HBT, mp 159−160 °C). ^{1}H NMR (200 MHz, chloroform-*d*): δ 3.84 (s, 18H), 6.90 and 7.36 (dd, J = 8.9 Hz, 24H), 7.81 (s, 6H). ^{13}C NMR (50 MHz, chloroform-*d*): δ 55.66, 115.4, 124.70, 125.4, 128.1, 134.8, 138.2, 160.0.

Crystallization of HPhTT·AgBF$_4$ (1a). Tetrahydrofuran (THF) solutions of HPhTT (4.3mM, 1.0 mL) and $AgBF_4$ (6.4 mM, 1.0 mL) were first mixed in a small vial, and hexafluorobenzene (HFB, 2 mL) was added to produce a white precipitate. Enough acetone (about 2 mL) was then added to dissolve the precipitate, and the resultant yellowish solution (in the same small vial, loosely capped) was placed into a larger vial containing a reservoir of hexanes (about 20 mL). The larger vial was tightly capped and placed in the dark to form blocklike light yellow single crystals over a period of 14 days. Larger single-phase samples can be obtained by similar setups on a larger scale. For example, HPhTT (15.2 mg, 17.4 μmol) and $AgBF_4$ (5.1 mg, 26.2 μmol) were similarly mixed with THF (5.0 mL), HFB (5.0 mL), and acetone (5 mL) and divided into three vials, which were then loosely capped and placed into a jar containing hexanes for slow crystallization. After about 2 weeks, the crystals were filtered and rinsed with hexanes (12.6 mg, 77% based on HPhTT). X-ray powder diffraction indicated a single phase consistent with the single-crystal structure (see Figure S1 in the Supporting Information). Solution ^{1}H NMR spectroscopy in CD_2Cl_2/CD_3CN (1:1) of the as-synthesized crystalline sample indicated a 2:1:1 ratio of HPhTT (e.g., δ 7.99, 12H), THF (e.g., δ 3.67, 4H), and acetone (δ 2.11, 6H). To test the framework stability as well as the volatility of the included solvent molecules (THF and acetone), the as-synthesized sample was heated at 180 °C for 20 min, and the resultant solid sample was studied by powder X-ray diffraction (sample pressed onto a glass slide for data collection at room temperature in air; see also Figures S2 and S3 in the Supporting Information) and solution ^{1}H NMR spectroscopy (solid sample dissolved in 1:1 CD_2Cl_2/CD_3CN; no peaks for THF or acetone were observed).

Crystallization of HPhTT·AgTf (1b). Toluene solutions of HPhTT (6.4 mM, 0.3 mL) and AgTf (9.7 mM, 0.3 mL) were first mixed in a glass tube (10-mm o.d./6-mm i.d.), and HFB (0.2 mL) and acetone (0.1 mL) were subsequently added to provide a colorless solution. After sequentially layering toluene (0.4 mL) and hexane (1.0 mL) on top of the solution, the tube was sealed and kept in the dark. Colorless, blocklike crystals suitable for X-ray studies were obtained after 1 week. Larger bulk samples can be obtained by similar setups on a larger scale (yield 65% based on

HPhTT). X-ray powder diffraction indicated a single phase consistent with the single-crystal structure (see Figure S4 in the Supporting Information).

Crystallization of HMOPhTT·AgSbF$_6$ (2). Single crystals suitable for X-ray data collection were first obtained as follows: Toluene solutions of HMOPhTT (2.3 mM, 0.4 mL) and $AgSbF_6$ (3.3 mM, 0.4 mL) were mixed in a small vial to give a turbid solution. Hexafluorobenzene (0.4 mL) was then added, and more white precipitate was formed as a result. Acetone (4.0 mL) was then added to dissolve the precipitate, and the vial containing the resultant solution was loosely capped and placed into a larger vial containing heptane. The larger vial was tightly capped and placed in the dark for slow crystallization. Chunky, blocklike, light yellow single crystals formed after about 14 days (yield 56% based on HMOPhTT). The crystalline product can also be made in the following way: HMOPhTT (14.5 mg, 13.7 μmol) was dissolved in a solvent mixture of 1:2:1 toluene/HFB/acetone (total of 2.0 mL, equivalent to 7.4 mM). The light yellow solution was then evenly divided and loaded into five glass tubes (5-mm i.d.) and layered sequentially with toluene (one-half of the volume of the HMOPhTT solution) and an acetone solution of $AgSbF_6$ (7.6 mM, same volume as the HMOPhTT solution in each tube). The glass tubes were then sealed and placed in the dark. Crystals formed after 2 weeks (17.2 mg collected from four of the tubes, 55% yield based on HMOPhTT). X-ray powder patterns of this bulk sample indicated a single phase consistent with the single-crystal structure (see Figure S5 in the Supporting Information). To further verify the chemical composition of the solid sample, the crystals were dissolved in 2:1 CD_2Cl_2/DMSO-d_6 for ^{1}H NMR measurements, which indicated a 1:4 molar ratio between the included acetone guest and the HMOPhTT molecule. ^{1}H NMR: δ 2.11 (s, 6H, acetone), 3.85 (s, 72H), 6.95 (d, 48H, J = 8.0 Hz), 7.37 (d, 48H, J = 8.0 Hz), 7.80 (s, 24H). Chemical analysis of the crystals (according to the formula HMOPhTT·$AgSbF_6$·0.25acetone as indicated by solution ^{1}H NMR spectroscopy) yields the following: calcd C 51.55%, H 3.52%; found C 51.25%, H 3.51%.

X-ray Single-Crystal Diffraction Studies of HPhTT·AgBF$_4$ (1a). A colorless block with dimensions 0.52 × 0.50 × 0.38 mm^3 was placed and optically centered on a Bruker SMART CCD system at 173 K. A total of 45690 reflections were collected and corrected for Lorentz and polarization effects and absorption using Blessing's method as incorporated into the program SADABS[53,54] with 11728 unique reflections. The SHELXTL[55] program package was employed to determine the probable space group and set up the initial files. System symmetry, systematic absences, and intensity statistics indicated the Laue class 4/m. The structure was solved by direct methods (with the successful location of nearly a complete molecule) in the noncentrosymmetric space group $I\bar{4}$ and subsequently refined with SHELXL 97. The BF_4^- anion was refined over three sets of disordered positions, with the associated occupancy factors refined as free variables. Two fragments suggestive of the acetone molecules (included solvent molecules) were also located from the Fourier map and each refined over two sets of disordered positions. All non-hydrogen atoms except those of the anions and the solvent molecules were refined anisotropically. All hydrogen atoms were placed in calculated positions without further refinement. The data for the crystal structure of **1b** were similarly collected and processed. Selected crystallographic results are summarized in Table 1, and full details of the crystallographic studies are included in the Supporting Information.

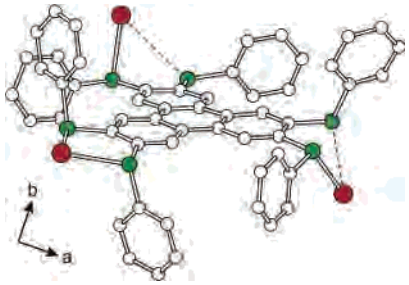

Figure 1. Conformation of the HPhTT molecules and the associated Ag^+ ions in the crystal structure of **1a**. Red sphere, Ag^+; green sphere, S; white sphere, C.

X-ray Single-Crystal Diffraction Studies of HMOPhTT·AgSbF$_6$ (2). A colorless block with dimensions 0.40 × 0.32 × 0.25 mm^3 was placed and optically centered on a Rigaku Mercury CCD area detector employing graphite-monochromated Mo Kα radiation (λ = 0.71069 Å) at 143 K. Rotation images were processed using CrystalClear (Rigaku Corporation, 1999), producing a listing of unaveraged F^2 and $\sigma(F^2)$ values that were then passed to the CrystalStructure program package (Rigaku Corp., Rigaku/MSC, 2002) for further processing and structure solution on a Dell Pentium III computer. The intensity data were corrected for Lorentz and polarization effects and for absorption using REQAB.[56] The structure was solved by direct methods (SIR97).[57] Refinement was done by full-matrix least-squares based on F^2 using SHELXL-97 (G. M. Sheldrick, University of Göttingen, Göttingen, Germany, 1997). An isolated fragment indicative of the included acetone molecule was located from the Fourier map, but was refined isotropically (mainly due to the relatively large Debye−Waller factors) with one-half occupancy as suggested by the compositions determined from solution NMR spectroscopy (see above). The hydrogen atoms were refined using a "riding" model. Selected crystallographic results are summarized in Table 1, and full details of the crystallographic studies are included in the Supporting Information.

Results and Discussion

Single-Crystal Structure and Property Studies of HPhTT·AgBF$_4$ (1a). This structure was refined in the noncentrosymmetric space group $I\bar{4}$, with one HPhTT molecule and one $AgBF_4$ unit contained in the asymmetric portion of the unit cell. The coordination between the HPhTT ligand and the Ag(I) atoms results in a 3D network with the 8^2·10-*a* topology,[58] which has remained relatively rare among reported coordination frameworks.[59,60] The HPhTT ligand adopts an irregular, star-shaped conformation (point-group symmetry C_1), and the sulfur atoms form coordination (chelation) bonds to the Ag(I) atoms, as shown in Figure 1. The overall coordination environment of the Ag(I) atom

(53) Blessing, R. H. *Acta Crystallogr. A: Found. Crystallogr.* **1995**, *A51*, 33.
(54) Sheldrick, G. M. *SADABS: Siemens Area Detector Absorption Correction*; Universität Göttingen: Göttingen, Germany, 1996.
(55) Sheldrick, G. M. *SHELXTL/PC*, version 5.03; Siemens Analytical X-ray Instruments Inc.: Madison, WI, 1994.
(56) Jacobson, R. A. Department of Chemistry, Iowa State University, Ames, IA; private communication, 1994.
(57) Altomare, A.; Burla, M. C.; Camalli, M.; Cascarano, G. L.; Giacovazzo, C.; Guagliardi, A.; Moliterni, A. G. G.; Polidori, G.; Spagna, R. *J. Appl. Crystallogr.* **1999**, *32*, 115.
(58) Wells, A. F. *Three-Dimensional Nets and Polyhedra*; Wiley-Interscience: New York, 1977.
(59) Dai, J.-C.; Wu, X.-T.; Fu, Z.-Y.; Hu, S.-M.; Du, W.-X.; Cui, C.-P.; Wu, L.-M.; Zhang, H.-H.; Sun, R.-Q. *Chem. Commun.* **2002**, 12.
(60) Wu, T.; Yi, B.-H.; Li, D. *Inorg. Chem.* **2005**, *44*, 4130.

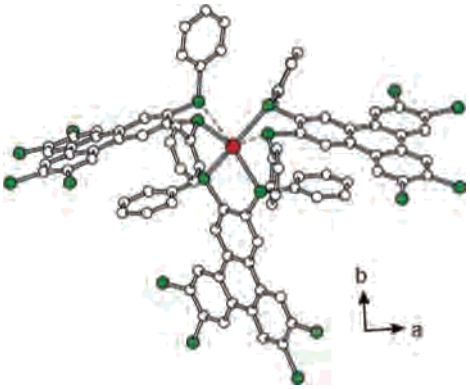

Figure 2. Coordination environment around the Ag(I) atom in the crystal structure of **1a**. Red sphere, Ag(I); green sphere, S; white sphere, C.

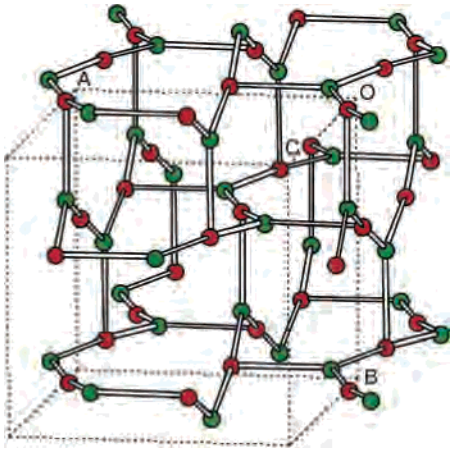

Figure 3. Schematic representation of the 8^2•10-*a* net in **1a**. Red sphere, Ag; green sphere: geometric center of the HPhTT triphenylene unit.

involves six sulfur atoms from three HPhTT molecules (see Figure 2). Four of the Ag−S bonds are relatively short (bond lengths 2.546, 2.578, 2.666, and 2.695 Å), and they constitute a distorted tetrahedral geometry around the Ag(I) atom; the other two Ag−S contacts are significantly longer (bond lengths 3.118 and 3.566 Å), completing a distorted octahedron as the overall geometry around the Ag(I) atom.

The 8^2•10-*a* topology of the coordination network is best visualized by a simplified net consisting of two distinct three-connected nodes (i.e., Ag^+ and the geometric center of HPhTT triphenylene core; see Figure 3). The HPhTT node features an almost ideal trigonal-planar connection to three neighboring Ag(I) nodes, whereas the connection around Ag(I) node is distorted, resembling a T shape instead of the trigonal-planar geometry. The projection along the 4-fold axis (i.e., the crystallographic *c* axis; Figure 4) provides a top view of the 4-fold helices and their relative chiralities: the helices are arranged in a square grid, with the closest neighbors being of opposite chirality and the diagonal neighbors being of identical chirality.

The overall crystal structure features two types of channels along the *c* axis with distinct sizes in diameters (Figure 5). The small channel is occupied by the BF_4^- anion, whereas the large channel contains the solvent molecules (e.g., THF and acetone) incorporated in the crystallization process. Calculation using the PLATON program[61] shows that up to 16.5% of the unit cell volume is potentially solvent-

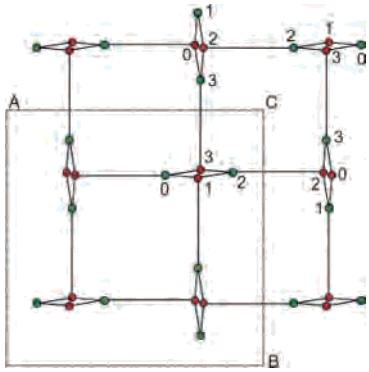

Figure 4. View along the 4-fold helices of the 8^2•10-*a* net in **1a**. The numbers indicate the relative heights above the page. Red sphere, Ag; green sphere, geometric center of the HPhTT triphenylene unit.

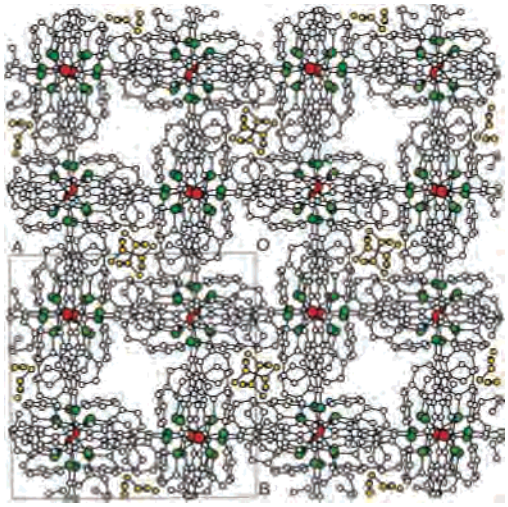

Figure 5. View of the crystal structure of **1a** along the *c* axis. Red sphere, Ag; green sphere, S. The disordered BF_4^- anion is colored orange.

accessible. Solution ^{1}H NMR spectra (in 1:1 CD_2Cl_2/CD_3CN) of an as-synthesized crystalline sample indicated a 1:1:2 molar ratio of THF, acetone, and the HPhTT molecule.

To test the stability of the host network, another as-synthesized sample of **1a** was heated at 180 °C for 20 min, and the resultant sample was studied by solution ^{1}H NMR spectroscopy and X-ray powder diffraction. Whereas solution ^{1}H NMR spectroscopy (in 1:1 CD_2Cl_2/CD_3CN) shows virtually complete removal of the acetone and THF molecules, X-ray powder diffraction indicates that the crystalline framework was maintained in the evacuated sample (see Figures S2 and S3 in the Supporting Information). Thus, a stable and crystalline apohost of the coordination network of **1a** has been achieved, and further studies on diffusion and adsorption properties in the solid state are ongoing.

No aromatic $\pi-\pi$ stacking arrangement is observed between the triphenylene units. Instead, both sides of the triphenylene plane are π-stacked in a face-to-face manner with side-chain phenyl groups from neighboring HPhTT molecules (interplanar distances 3.43 and 3.46 Å; see Figure S6 in the Supporting Information), thus partially eclipsing the triphenylene π system from the channels of the framework structure. Although additional experimental studies on

(61) Spek, A. L. *J. Appl. Crystallogr.* **2003**, *36*, 7.

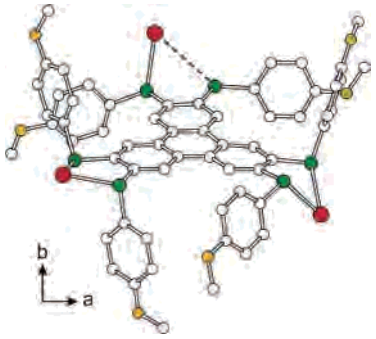

Figure 6. Conformation of an HMOPhTT molecule and the associated Ag^+ ions in the crystal structure of **2**. Red sphere, Ag^+; green sphere, S; orange: O; white, C.

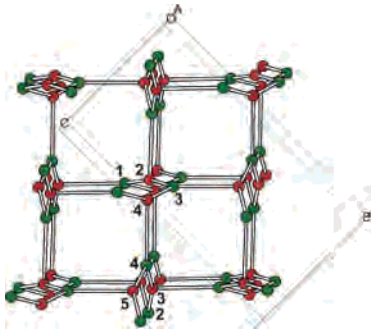

Figure 7. Schematic representation of the $8^2 \cdot 10$-*a* net in **2**. Red sphere, Ag; green sphere, geometric center of the HMOPhTT triphenylene unit.

the porous properties of this compound are ongoing, less-obstructed and guest-accessible triphenylene units, together with larger pore sizes, might be more desirable, if significant electronic impact (e.g., oxidative doping) of the triphenylene π system were to be achieved from guest diffusion experiments within the porous solid. The single-crystal structure of HPhTT·AgTf (**1b**) features a 3D network with the same topology as **1a**, and the local bonding features between the HPhTT molecules and the Ag^+ ions are also very similar.

Single-Crystal Structure and Property Studies of HMOPhTT·AgSbF$_6$ (2). Despite the rather extensive modification of the pendant phenyl groups, this structure continues to adopt the $8^2 \cdot 10$-*a* topology in the coordination network, with local bonding environments for the HMOPhTT ligand and the Ag(I) atom also being similar to those in **1a** and **1b** (Figures 6 and 7). However, the crystal structure here forms in a lower-symmetry monoclinic system with the noncentrosymmetric space group *Cc*, with the asymmetric portion of the unit cell containing two HMOPhTT molecules and two $AgSbF_6$ moieties. The conformations of the two crystallographically inequivalent HMOPhTT molecules are very similar, as are the coordination environment around the two Ag(I) atoms (distorted octahedral, with Ag−S distances of 2.569, 2.583, 2.589, 2.620, 2.636, 3.010, and 3.583 Å for Ag1 and 2.546, 2.614, 2.623, 2.817, 2.841, and 3.338 Å for Ag2; see also Figures S7 and S8 in the Supporting Information). Crystallographic analysis located one fragment for acetone (one of the solvents for the crystal growth) in the asymmetric portion of the unit cell, with solution ^{1}H NMR spectroscopy indicating a 1:4 molar ratio of the acetone and

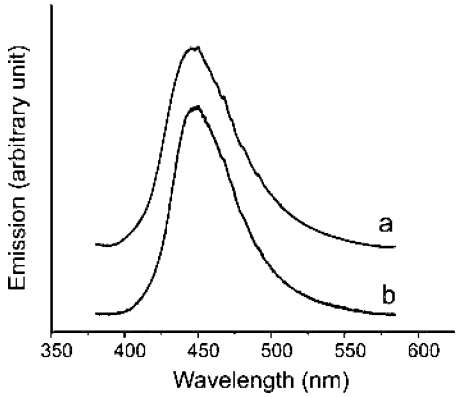

Figure 8. Room-temperature solid-state emission spectra of (a) **1a** and (b) **2** (excitation wavelength $\lambda_{ex} = 300$ nm).

the HMOPhTT molecule. Volume calculation using PLATON indicates virtually no solvent-accessible space besides that of the acetone guests.

Fluorescence measurements of the solid samples (e.g., **1a** and **2**) indicated that the fluorescent properties of the triphenylene core are maintained in the 3D networks. Specifically, both **1a** and **2** show a distinct fluorescence band with $\lambda_{F,max} = 450$ nm at room temperature, with the overall features of the fluorescence spectra also being quite similar (Figure 8). Compound **1a**, with its robust porous structure, presents a particularly interesting system for studying impacts of guest molecules on the fluorescence properties of the host network and for probing potential applications in solid-state fluorescent sensing.

Taken together, the above studies indicate that the polycyclic aromatic triphenylene group has been integrated into three 3D metal−organic coordination networks. Of particular interest is compound **1a** (and probably the isostructural **1b** as well), which features a porous framework with substantial thermal stability. The highly polarizable π electrons on the triphenylene unit and the associated fluorescent properties might offer attractive opportunities for studying further materials chemistry and properties in this well-defined porous medium.

Acknowledgment. This work was partially supported by City University of Hong Kong (Projects 9360121 and 7200041). We thank George Washington University's University Facilitating Fund and donors of the American Chemical Society Petroleum Research Fund for partial support of this research. Z.X. is a recipient of the 2004 Ralph E. Powe Junior Faculty Enhancement Award. We also thank our undergraduate member, Ms. Rachel Mednick, for participating in this project.

Supporting Information Available: Full crystallographic data in CIF format for compounds **1a**, **1b**, and **2**. Additional figures of the crystal structures of **1a**, **1b**, and **2**. X-ray powder diffraction patterns for bulk samples of **1a**, **1b**, **2**, and an apohost sample of **1a**. This material is available free of charge via the Internet at http://pubs.acs.org.

IC051135E